Journal of Power Sources 330 (2016) 175–185

Contents lists available at ScienceDirect

Journal of Power Sources

journal homepage: www.elsevier.com/locate/jpowsour

The effectiveness of electrolyte additives in fluorinated electrolytes for high voltage $Li[Ni_{0.4}Mn_{0.4}Co_{0.2}]O_2$/graphite pouch Li-ion cells

Jian Xia [a], R. Petibon [b], A. Xiao [c], W.M. Lamanna [c], J.R. Dahn [a, b, *]

[a] Dept. of Physics and Atmospheric Science, Dalhousie University, Halifax, Nova Scotia, B3H3J5, Canada
[b] Dept. of Chemistry, Dalhousie University, Halifax, Nova Scotia, B3H3J5, Canada
[c] Electronic Materials Solutions Division, 3M Co., 3M Center, St. Paul, MN, USA

HIGHLIGHTS

- Fluorinated electrolytes with electrolyte additives were studied.
- Additives such DTD and MMDS improved the cycling performance.
- Fluorinated electrolytes show gassing and impedance growth even with additives.

GRAPHICAL ABSTRACT

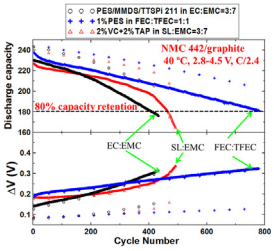

ARTICLE INFO

Article history:
Received 12 June 2016
Received in revised form
11 August 2016
Accepted 3 September 2016
Available online 10 September 2016

Keywords:
High voltage lithium-ion batteries
Fluorinated electrolytes
Limiting gas evolution
Electrolyte additives
Limiting impedance growth

ABSTRACT

The effectiveness of electrolyte additives in fluorinated electrolytes containing 1 M $LiPF_6$/fluoroethylene carbonate:bis (2,2,2-trifluoroethyl) carbonate (1:1 w:w) were studied in high voltage $Li(Ni_{0.4}Mn_{0.4}Co_{0.2})O_2$/graphite pouch cells tested to 4.5 V. The results showed that fluorinated electrolytes containing prop-1-ene-1,3-sultone alone or in combination with other additives exhibited significant improvements in terms of coulombic efficiency and charge endpoint capacity slippage during UHPC cycling, voltage drop during storage, as well as capacity retention during long-term cycling compared with state-of-the-art ethylene carbonate-based (ethylene carbonate: ethylmethyl carbonate 3:7) or sulfolane-based electrolytes (sulfolane: ethylmethyl carbonate 3:7) with some promising additive blends. These results indicate that fluorinated electrolytes offer an interesting alternative for high voltage Li-ion batteries.

1. Introduction

Li-ion cells with high energy density as well as long life-time are desired for electric vehicles and grid energy storage. While many researchers have been focusing on the development of positive and negative electrode materials with higher specific capacities or positive electrode materials with higher average voltage, less attention has been paid to the advancement of the electrolyte. Recent studies [1–3] demonstrated that using a combination of electrolyte additives can greatly increase the cycle life time of Li-ion cells. A long-term cycling study of electrolyte additives in $Li[Ni_{1/3}Mn_{1/3}Co_{1/3}]O_2$ (NMC111)/graphite pouch cells operated to 4.2 V showed the beneficial effect of using combinations of additives instead of electrolytes with only one additive [4]. However, recent work presented by Ma et al. showed that the benefit brought by electrolyte additives in traditional carbonate electrolyte in cells cycled at or above 4.5 V is diminished [5]. This is because electrolyte

* Corresponding author. Dept. of Physics and Atmospheric Science, Dalhousie University, Halifax, Nova Scotia, B3H3J5, Canada.
E-mail address: jeff.dahn@dal.ca (J.R. Dahn).

http://dx.doi.org/10.1016/j.jpowsour.2016.09.012
0378-7753/

solvents (such as ethylene carbonate) and/or salts (such as $LiPF_6$) are unstable at high voltages and the positive electrode solid electrolyte interface (SEI) becomes less protective as the potential increases. The parasitic degradation of these components lead to gas evolution [6], salt consumption [7] as well as severe impedance growth [8] which limit the lifetime of lithium ion cells operated to high potential.

To solve this problem, researchers are searching for new alternative electrolyte solvents which have high anodic stability at high voltages. For example, Xu et al. [9,10] and Abouimrane et al. [11] developed sulfone-based electrolytes which exhibited excellent electrochemical stability and capacity retention for high voltage positive materials. Abu-Lebdeh et al. [12,13] and Nagahama et al. [14] showed that nitrile-based electrolytes have a wide electrochemical window up to 6 V vs Li^+/Li and when used with other solvents and salts can provide an interesting alternative for high voltage applications. However, sulfones and nitriles have problems with their high melting points, high viscosity and low dielectric constant as well as their inability to passivate graphite and solvate $LiPF_6$. As a result, these solvents were mainly investigated in cell systems containing Li metal or $Li_4Ti_5O_{12}$ as anodes [11,15,16] and with salts such as LiTFSI or LiBOB [12,17,18].

Fluorinated organic carbonates were studied by Moller et al. [19] and Smart et al. [20] to improve low temperature performance. Zhang et al. [21] showed that fluorinated carbonates have superior voltage stability towards the 5.0 V spinel $LiNi_{0.5}Mn_{1.5}O_4$ (LNMO) cathode and enhanced cycle stability compared to EC/EMC-based electrolytes in LNMO/Li and LNMO/$Li_4Ti_5O_{12}$ coin-type cells. However, poor capacity retention was observed in LNMO/graphite cell chemistry containing all-fluorinated electrolytes [22]. The cycling performance in LNMO/graphite cells was then improved by using a lithium reservoir [23] or by replacing fluorinated cyclic carbonate (F-AEC) with fluoroethylene carbonate (FEC) [24].

Enlightened by the above work of Zhang and Amine et al., we recently reported a fluorinated carbonate mixture composed of fluoroethylene carbonate (FEC) and bis(2,2,2-trifluoroethyl) carbonate (TFEC) with prop-1-ene-1,3-sultone (PES) as an electrolyte additive. The reason for choosing FEC and TFEC is that the cyclic carbonate (FEC) can help form the SEI on the negative electrode while the linear carbonate (TFEC) can help lower the viscosity and melting point of the electrolyte. Li[$Ni_{0.4}Mn_{0.4}Co_{0.2}$]O_2 (NMC442)/graphite pouch cells showed impressive cycling stability to 4.5 V using this electrolyte system [25]. Here, as a follow-up investigation, a series of electrolyte additive blends in the FEC:TFEC-PES electrolyte system have been studied in machine-made NMC442/graphite pouch type Li-ion cells. These electrolyte blends were evaluated using Ultra High Precision Coulometry (UHPC) [26], precision storage experiments [27], *ex-situ* gas volume evolution [28] as well as electrochemical impedance spectroscopy (EIS). Gas evolution during formation and cycling, coulombic efficiency, charge endpoint capacity slippage during cycling and EIS spectra before and after cycling were examined and compared with two other electrolyte systems including ethylene carbonate (EC):ethylmethyl carbonate (EMC) and sulfolane (SL):EMC. Long-term cycling results to 4.5 V were also made to compare the cycling stability of cells with these three electrolyte systems.

2. Experimental

2.1. Electrolyte and chemicals

1 M $LiPF_6$ EC:EMC (3:7 wt% ratio, BASF, 99.99%) was used as the control electrolyte. 1 M $LiPF_6$ SL:EMC (3:7 wt% ratio) was also used for comparison. The fluorinated electrolyte system studied consisted of 1 M $LiPF_6$ FEC:TFEC (1:1 w:w) + 2% PES to which various additives were added. The solvent TFEC was obtained from HSC Corporation (Jiangsu, China, 99.80 wt%) while the FEC was from BASF (99.94 wt%). The conductivity as a function of temperature of the three electrolyte systems is shown in Fig. 1. Fig. 1 shows that 1 M $LiPF_6$ in FEC:TFEC (1:1) electrolyte has a lower conductivity than that of 1 M $LiPF_6$ EC:EMC (3:7) or 1 M $LiPF_6$ SL:EMC (3:7) electrolyte system throughout the whole temperature range tested (−30 °C–60 °C).

Additives were added in a 1–8 wt.% range to these three types of electrolytes. The additives selected for this study are well-known in the literature and have been shown to improve the quality of the negative electrode SEI or to reduce parasitic reactions at high voltage in NMC442/graphite cells. These additives included vinylene carbonate (VC), prop-1-ene,1,3-sultone (PES), methylene methane disulfonate (MMDS), ethylene sulfite (ES), propanediol cyclic sulfate (TMS), 1,3,2-dioxathiolan-2,2-oxide (DTD), tris trimethylsilyl phosphite (TTSPi) as well as triallyl phosphate (TAP). Fig. S1 (supporting information) shows the chemical structures of the additives that were studied in this paper. The reasons for choosing these additives have explained in Refs. [29–37]. As examples, VC [31] and PES [32] are SEI forming additives and gas reducers. MMDS [33], ES [34], TTSPi [35] have been shown to be effective impedance reducers. Both DTD [36] and TAP [37] can improve the coulombic efficiency (CE) and cycle life time. The additive TAP can be easily polymerized through a cross-linked electro-polymerization of its three allyl groups at the surface of both graphite and coated NMC442 electrodes, leading to higher cell impedance. The purities and the suppliers of the additives used are listed in Table S1 (supporting information). 2% PES + 1% MMDS (or DTD) + 1% TTSPi (PES211) in EC:EMC (3:7 wt%) electrolyte and 2% VC + 2% TAP in SL:EMC (3:7 wt%) were used for comparison in some of the experiments. The details of the PES211 additive combinations [5], tri-allyl phosphate (TAP) [37] and SL:EMC-VC electrolyte [38] have been reported in previous publications.

2.2. Pouch cells, cell formation and degassing

The pouch cells employed in this study were all Li[$Ni_{0.4}Mn_{0.4}Co_{0.2}$]O_2 (NMC442)/graphite cells with a capacity of 245 mAh having a negative electrode active mass and positive electrode active mass ratio balanced for 4.7 V operation. SEM images of the NMC442 and graphite electrodes are shown in Fig. S2 so that the reader can appreciate the morphology of the particles that make up the electrodes. The 402035-size pouch cells were manufactured by Li-Fun Technology (Xinma Industry Zone, Golden Dragon Road, Tianyuan District, Zhuzhou City, Hunan Province, PRC, 412000). The cells were balanced for 4.7 V operation and had a capacity of

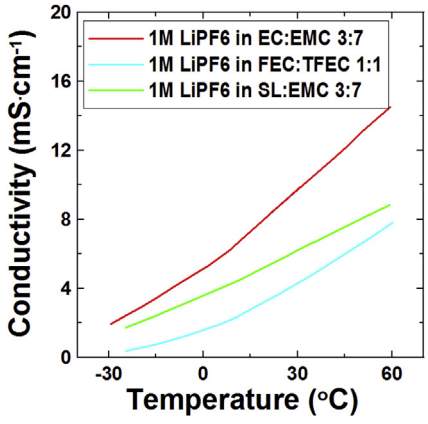

Fig. 1. Conductivity measurements of FEC:TFEC, SL:EMC and EC:EMC electrolytes.

245 mAh at 4.5 V, the maximum voltage used in this study. The negative electrodes of these cells were 95.4% artificial graphite particles (supplied by BTR New Materials Technology, 15–30 μm), 1.3% carbon black conductive diluent and 3.3% binder (carboxymethylcellulose (CMC)/styrene butadiene rubber (SBR)). The positive electrodes were 96.2% $Li[Ni_{0.4}Mn_{0.4}Co_{0.2}]O_2$ (NMC442, supplied by Umicore, Korea) particles (5–15 μm), 1.8% carbon black conductive diluent and 2% polyvinylidene fluoride (PVDF) binder. The pouch cells were 40 mm long x 20 mm wide x 3.5 mm thick. The positive electrode had a total thickness of 105 μm and was calendared to a density of 3.55 g/cm^3. The negative electrode had a total thickness of 110 μm and was calendared to a density of 1.55 g/cm^3. The positive electrode coating had an areal density of 16 mg/cm^2 (one side) and the negative electrode had an areal density of 9.5 mg/cm^2 (one side). The positive electrode dimensions were 200 mm × 26 mm and the negative electrode dimensions were 204 mm × 28 mm. Both electrodes were coated on both sides, except for small regions on one side at the end of the foils leading to an active area of approximately 100 cm^2. The electrodes were spirally wound, not stacked, in these pouch cells. The pouch cells were vacuum sealed without electrolyte in China and then shipped to our laboratory in Canada. Before filling with electrolyte, the cells were cut just below the heat seal and dried at 80 °C under vacuum for 14 h to remove residual water. Then the cells were transferred immediately to an argon-filled glove box for filling and vacuum sealing. The NMC442/graphite pouch cells were filled with 0.75 mL of electrolyte. The electrolyte formulations as well as their volume, corresponding density and mass are shown in Table S2. After filling, cells were vacuum-sealed with a compact vacuum sealer (MSK-115A, MTI Corp.). First, cells were placed in a temperature box at 40.0 °C where they were held at 1.5 V for 24 h, to allow for the completion of wetting. Then, cells were charged at 12 mA (C/20) to 3.5 V. This step is called formation step 1. After formation step 1, cells were transferred into the glove box, cut open just below the seal to release any gas generated during the partial charge to 3.5 V and vacuum sealed again. These cells were then charged from 3.5 V at 12 mA (C/20) to 4.5 V. This step is called formation step 2. After formation step 2, the cells were transferred into the glove box, cut open to release gas generated and then vacuum sealed again. These degassing voltages were selected based on the in-situ gas evolution experiments that show most of the gas evolves in the formation step at voltages below 3.5 V and above 4.3 V [39]. After the two degassing processes, cells were then discharged to 3.8 V where their impedance spectra were measured.

2.3. UHPC and storage protocols

The cycling/storage procedure was carried out using the Ultra High Precision Charger (UHPC) at Dalhousie University [25]. Testing was performed between between 2.8 and 4.4 V at 40.0 ± 0.1 °C using cycling/storage protocols (Fig. S3). Cells were first charged to 4.400 V using currents corresponding to C/10, stored at open circuit at 4.400 V for 20.00 h and then discharged to 2.800 V using currents corresponding to C/10. This process was repeated on the UHPC for 15 cycles where comparisons were made. The cycling/storage procedure [38] was designed so that the cells were exposed to higher potentials for significant fractions of their testing time. For storage experiments, cells were first discharged to 2.8 V and charged to 4.5 V twice. Then the cells were held at 4.5 V until the measured current decreased to 0.0025 C. A Maccor series 4000 cycler was used for the preparation of the cells prior to storage. After the pre-cycling process, cells were carefully moved to the storage system which monitored their open circuit voltage every 6 h for a total storage time of 500 h [40]. Storage experiments were made at 40.0 ± 0.1 °C.

2.4. Ex-situ gas measurements

Ex-situ gas measurements were made by suspending pouch cells from a fine wire "hook" attached under a Shimadzu balance (AUW200D) [28]. The pouch cells were immersed in a beaker of deionized "nanopure" water (18 MΩ) that was at 20 ± 1 °C for measurement. Before weighing, all cells were charged or discharged to 3.80 V. The changes in the weight of the cell suspended in fluid, before, during and after testing are directly related to the volume changes by the change in the buoyant force. The change in mass of a cell, Δm, suspended in a fluid of density, ρ, is related to the change in cell volume, Δv, by

$$\Delta v = -\Delta m/\rho \quad (1)$$

2.5. Electrochemical impedance spectroscopy

Electrochemical impedance spectroscopy (EIS) measurements were conducted on NMC442/graphite pouch cells after formation and also after cycling on the UHPC. Cells were charged or discharged to 3.80 V before they were moved to a 10.0 ± 0.1 °C temperature box. Alternating current (AC) impedance spectra were collected with ten points per decade from 100 kHz to 10 mHz with a signal amplitude of 10 mV at 10.0 ± 0.1 °C. A Biologic VMP-3 was used to collect these data. The experimental setup did not allow for reproducible solution resistance measurements due to cable and connector impedance. Therefore, all impedance spectra were shifted to 0 on the real axis at the highest frequency measured.

2.6. Long term cycling

After formation, cells were continuously cycled between 2.8 V and 4.5 V at 40 ± 0.5 °C using currents corresponding to C/2.4 (100 mA). The cells were sandwiched between two rectangular silicone rubber pieces (McMaster-Carr part number 5508T45) placed in the cell holder with aluminum shims added to ensure firm pressure [38]. With the clamps in place, gas is pushed to the edges of the pouch where there is ample space for it and the clamps maintain stack pressure on the cell. A low rate C/10 cycle was included every 50 cycles to gauge what fraction of the capacity loss was due to impedance growth during the high rate cycling.

3. Results and discussion

Fig. 2 shows typical data collected during some of these experiments. Three electrolyte systems with different electrolyte additive combinations including 2% PES + 0.5% MMDS in the FEC:TFEC 1:1 electrolyte system, 2% VC + 2% TAP in the SL:EMC 3:7 electrolyte system and 2% PES + 1% MMDS + 1% TTSPi in the EC:EMC 3:7 electrolyte system were selected for comparison. The reason for choosing these three electrolyte formulations for display is based on their excellent cycling performance. Fig. 2a shows typical open circuit voltage (OCV) versus time during 500 h storage at 40.0 ± 0.1 °C for NMC442/graphite cells with the three electrolyte systems. Voltage drop (V_{drop}) during storage results directly from electrolyte oxidation at the surface of the positive electrode and has been shown to correlate well with charge endpoint capacity slippage [36]. That is, cells with large charge endpoint capacity slippage during cycling normally have large voltage drops during storage. Fig. 2a shows that cells containing 2% PES + 0.5% MMDS in FEC:TFEC 1:1 electrolyte have the smallest V_{drop} among the three electrolytes displayed.

Fig. 2b shows the coulombic efficiency (CE) versus cycle number

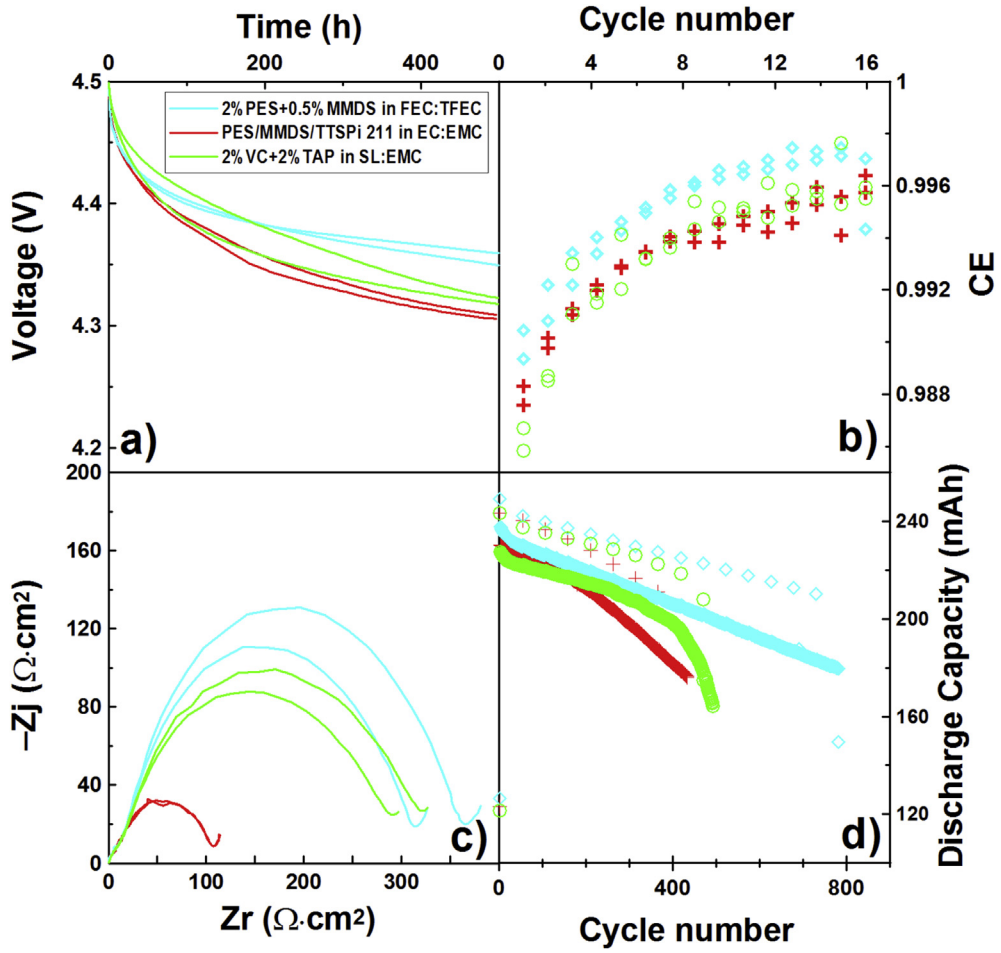

Fig. 2. a) Open circuit voltage versus time during 500 h storage at 40.0 °C; b) Coulombic efficiency during cycling/storage protocols on the UHPC at 40.0 °C, c) Nyquist plots after UHPC cycling and d) capacity vs cycle number during long-term cycling between 2.8 V and 4.5 V at 40. ±0.5 °C for NMC442/graphite pouch cells with different kinds of electrolyte solvents as indicated. Fig. 2 gives example data showing the methods used in this paper. The cycling/storage protocols are shown in Fig. S3. The curves marked in cyan, red and green in Fig. 3 represent cells containing FEC:TFEC, EC:EMC and SL:EMC electrolyte, respectively. (For interpretation of the references to colour in this figure legend, the reader is referred to the web version of this article.)

for cells with these three electrolyte systems tested at 40.0 °C during the cycling/storage protocol on the UHPC. The details of the cycling/storage protocol have been explained in Ref. [30] and are shown in Fig. S3 (supporting information). Fig. 2b shows that cells with 2% VC + 2% TAP in SL:EMC electrolyte have similar CE to the cells with 2% PES + 1% MMDS + 1% TTSPi in EC:EMC electrolyte. Fig. 2b shows that cells containing 2% PES + 0.5% MMDS in FEC:TFEC 1:1 electrolyte have higher CE than the other two electrolytes, which suggests such cells would have longer lifetime [3] when tested in this potential window as is evident in Fig. 2d.

Fig. 2c shows the impedance spectra measured after UHPC cycling. The EIS measurements were made at 10.0 °C and 3.80 V. The diameter of the semicircle represents the sum of the charge-transfer resistances, R_{ct}, at both the positive and negative electrodes. In this work, R_{ct} includes the active particle-current collector contact resistance of both electrodes (small), the resistance to the transfer of Li^+ from the electrolyte to the electrode through the solid electrolyte interface (SEI) of both electrodes, and the electron transfer to the active material of both electrodes [41]. Smaller values of R_{ct} are desired for these cells cycled during the same period of time. Fig. 2c shows that cells containing 2% PES + 0.5% MMDS in FEC:TFEC 1:1 electrolyte and 2% VC + 2% TAP in SL:EMC electrolyte have similar R_{ct} after UHPC cycling. However, cells containing both these EC-free electrolytes have much higher impedance than cells containing 2% PES + 1% MMDS + 1% TTSPi in EC:EMC electrolyte after UHPC cycling as expected based on the results in Fig. 2b.

Fig. 2d shows the capacity versus cycle number for the NMC442/graphite pouch cells containing the three different electrolytes during long-term cycling. The long-term cycling cells were cycled between 2.8 V and 4.5 V at 40 ± 0.5 °C using currents corresponding to C/2.4 (100 mA). Fig. 2d shows that cells containing 2% PES + 0.5% MMDS in FEC:TFEC 1:1 electrolyte have the best capacity retention among cells with the three electrolytes as expected based on Fig. 2b.

Fig. 3 summarizes the cycling data collected with the UHPC for NMC442/graphite pouch cells at 40.0 ± 0.1 °C with FEC:TFEC, SL:EMC and EC:EMC electrolyte systems with selected additives. The cells were tested with the charge-store-discharge protocol described in the experimental section to 4.4 V. Each data point in Fig. 3 represents the average of two cells and the error bars are the standard deviation of the results. The bars marked in cyan, red and green in Fig. 3 represent cells containing FEC:TFEC, EC:EMC and SL:EMC electrolyte, respectively. Fig. 3a summarizes the coulombic inefficiency (CIE = 1−CE) measured with the UHPC on cells with the electrolyte and additives as indicated. Detailed coulombic efficiency vs cycle number data for cells containing FEC:TFEC-based electrolytes are given in Figs. S4a, S5a and S6a in the supporting

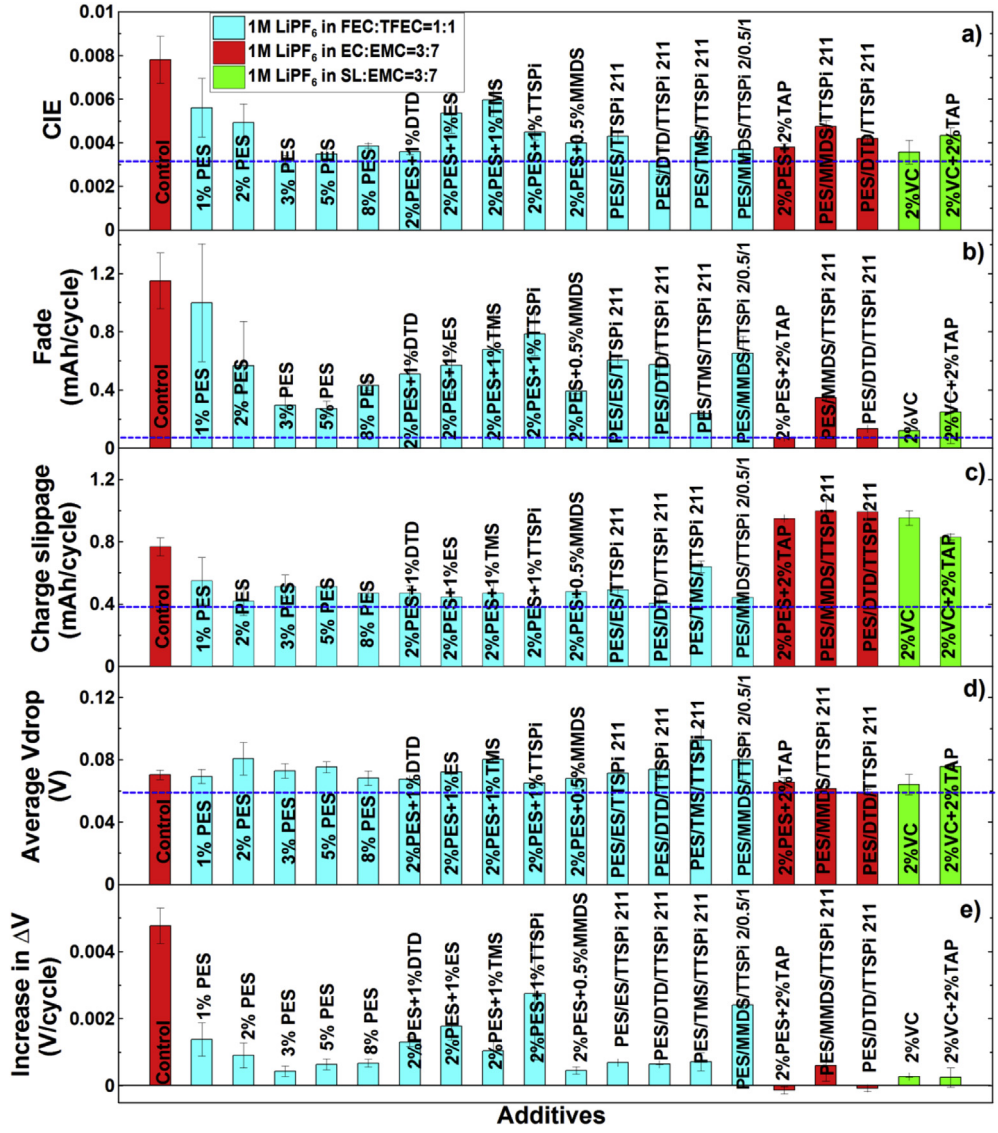

Fig. 3. Summary of cycling data collected on the UHPC including: CIE, the charge endpoint capacity, V_{drop} and ΔV for NMC442/graphite pouch cells in FEC:TFEC, SL:EMC and EC:EMC electrolytes using the cycling/storage protocols shown in Fig. S3. Cells were tested at 40.0 °C. The blue line represents the lowest value of all electrolytes tested. (For interpretation of the references to colour in this figure legend, the reader is referred to the web version of this article.)

information. The CIE was calculated from the CE taken as an average of the final three data points (cycles 13–15) collected on the UHPC. Just as a reminder, smaller values of CIE mean the cells had higher CE and should have a longer cycle and calendar life [3]. Fig. 3a shows that increasing the PES loading from 1 to 3% in FEC:TFEC electrolytes generally leads lower CIE (higher CE). Adding DTD or MMDS to FEC:TFEC + 2% PES electrolyte decreases the CIE while adding ES or TMS increases the CIE. Adding a third additive (TTSPi) to FEC:TFEC electrolyte further decreases the CIE, which agrees well with results shown by Sinha et al. [42]. Compared to electrolytes (EC-based and sulfolane-based) containing "PES 211" or 2% PES + 2% TAP additive combinations, most cells containing FEC:TFEC provide better CE during the 600 h of UHPC cycling.

Fig. 3b summarizes the capacity fade rate measured using the UHPC for NMC442/graphite pouch cells with different solvent blends and additive combinations at 40.0 ± 0.1 °C. Detailed discharge capacity vs cycle number data for cells containing FEC:TFEC electrolyte are given in Figs. S4b, S5b and S6b in the supporting information. The fade rate was calculated from the slope of a best fit line to the final five points (cycles 11–15) of the discharge capacity versus cycle number curves. The fade rate is caused by the depletion of the lithium inventory due to SEI growth at the negative electrode which was shown to be relatively independent of the upper cutoff voltage [43]. Fig. 3b shows that all of the cells containing FEC:TFEC electrolyte have higher fade rate than cells containing EC:EMC or SL:EMC electrolyte (except control cells), indicating that FEC:TFEC electrolyte has more rapid SEI growth on the negative electrode which causes the consumption the active Li.

Fig. 3c summarizes the charge endpoint capacity slippage measured using the UHPC for NMC442/graphite pouch cells with different solvent blends and additive combinations at 40.0 ± 0.1 °C. Detailed charge endpoint capacity vs cycle number data for cells containing FEC:TFEC-based electrolyte are given in Figs. S4c, S5c and S6c in the supporting information. The charge endpoint capacity slippage was calculated from the slope of a best fit line to the final five points (cycles 11–15) of the charge endpoint capacity versus cycle number curves. Fig. 3c shows that cells containing

SL:EMC electrolyte have similar charge end-capacity slippage rate to EC:EMC containing cells. Charge endpoint capacity slippage is caused by electrolyte oxidation reactions at the positive electrode which can cause impedance growth and/or eventually deplete the cell of electrolyte leading to cell failure [44]. Smaller charge endpoint capacity slippage rates are better. Fig. 3c shows that all of the cells containing FEC:TFEC electrolyte have much smaller charge endpoint capacity slippage rate than cells containing EC:EMC or SL:EMC electrolyte with or without additives, indicating that FEC:TFEC electrolyte has slowed electrolyte oxidation on the positive side. Fig. 3c also shows that adding additives to FEC:TFEC electrolyte does not strongly impact the charge endpoint capacity slippage rate.

Fig. 3d and e summarize V_{drop} during the storage portion of the UHPC testing and the average rate of increase in charge discharge polarization ΔV/cycle for the NMC442/graphite pouch cells with different additives combination at 40.0 ± 0.1 °C. Detailed V_{drop} and ΔV vs. cycle number data for cells containing FEC:TFEC-based electrolyte are given in Figs. S4d, S5d, S6d, S4e, S5e and S6e, respectively, in the supporting information. The average V_{drop} was calculated from an average of the final three data points (cycles 13–15) collected on the UHPC. The rate of increase of ΔV was calculated from the slope of a best fit line to the final five points (cycles 11–15) of the ΔV vs. cycle number curves. The differences in V_{drop} from cell to cell are caused by differences in the rate of the electrolyte oxidation on the positive side and also by differences in DC resistance which affect the rapid voltage change when the cells switch from charge to open circuit [30]. The increase in ΔV/cycle is caused by an increase in cell polarization during cycling and smaller values of ΔV/cycle generally indicate lower impedance growth during cycling [44]. Fig. 3d shows that cells containing FEC:TFEC electrolyte have higher V_{drop} than cells containing EC:EMC or SL:EMC electrolyte, indicating higher impedance during cycling. Fig. 3d shows the TAP-containing cells in EC:EMC or SL:EMC electrolytes have larger V_{drop} than TAP-free cells due to the high impedance caused by the polymerization of TAP [30]. The detailed voltage vs time curves during the last few cycles for some cells containing the three different kinds of electrolytes are given in Fig. S7. Fig. S7 shows that cells containing PES 211 in EC:EMC electrolyte have the smallest voltage drop during the last few cycles among the three types of electrolytes tested. Fig. 3e shows that the control cells have much larger values of ΔV/cycle, indicating remarkable impedance growth during the last few cycles on the UHPC. Fig. 3e shows cells containing FEC:TFEC electrolyte have larger impedance growth during UHPC cycling than cells containing EC:EMC or SL:EMC electrolytes.

Fig. S8 shows the capacity fade rate as a function of the increase in ΔV, both measured during UHPC cycling. Fig. S8 shows that the fade rate correlates well with the increase in ΔV. This suggests that at least a portion of the fade is due to impedance growth.

Fig. 4a shows the voltage drop during 500 h storage at 40.0 °C and 4.5 V. Storage data for all the cells containing FEC:TFEC

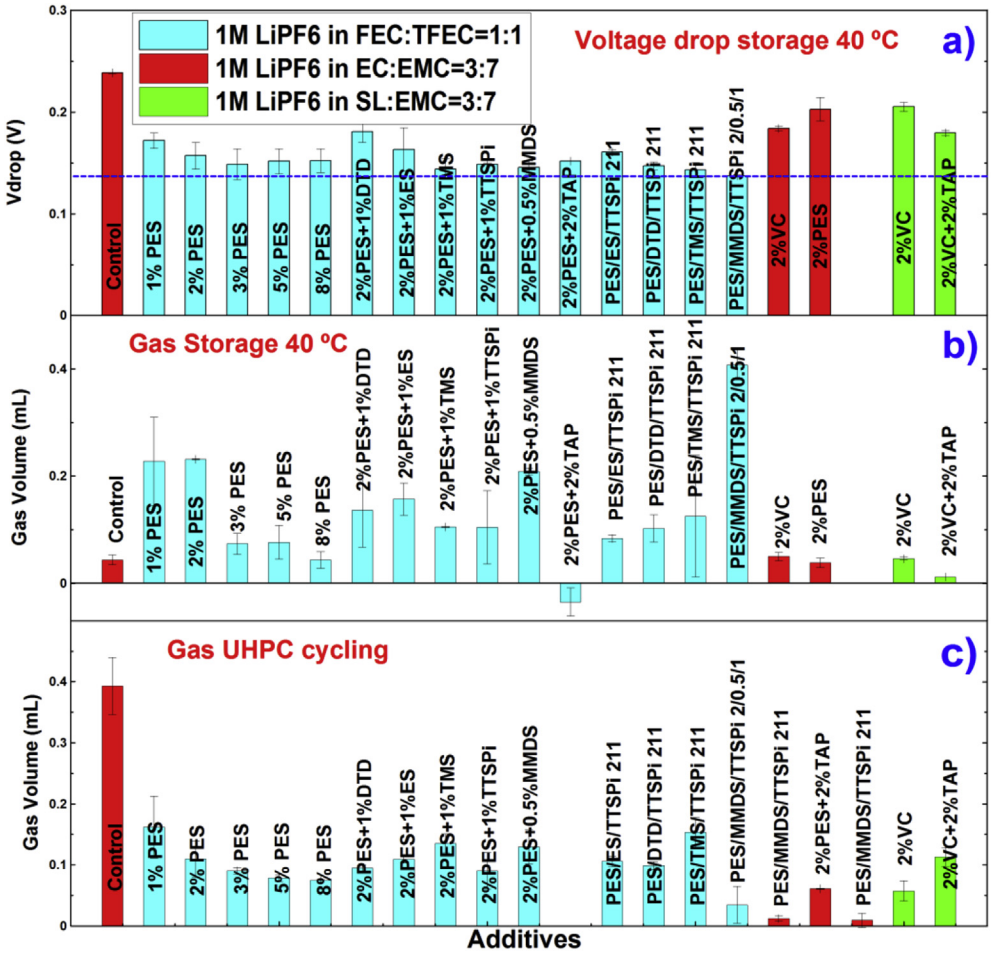

Fig. 4. Summary of a) the V_{drop} during 500 h storage at 40.0 °C, b) the gas evolution measured during 500 h storage at 40.0 °C and c) the gas evolution measured during UHPC cycling using the cycling/storage protocols shown in Fig. S3.

electrolytes tested in this study are given in Fig. S9. A smaller voltage drop indicates that cells have less electrolyte oxidation at the positive electrode during storage. Readers are reminded that there was a 24 h hold before the 500 h storage tests and therefore the voltage drop during storage is not caused by cell polarization, which is different than the voltage drop during UHPC tests. Fig. 4a shows that all of the cells containing FEC:TFEC electrolyte have smaller voltage drop than cells containing EC:EMC electrolyte or SL:EMC electrolyte. This agrees fairly well with the charge end-point capacity slippage results in Fig. 3b.

The gas produced during formation, during storage and during UHPC cycling was also measured. Minimizing the gas production in pouch cells is important because gas generation causes loss of stack pressure in the pouch, swelling and cell failure. Fig. S10 shows the gas produced during formation step 1 (charge to 3.5 V) and formation step 2 (charge to 4.5 V). Fig. S10 shows that cells containing FEC:TFEC electrolyte produced less gas than cells containing EC:EMC and SL:EMC electrolyte during both formation step 1 and formation step 2. Fig. 4b shows the volume of gas produced during 500 h storage for the same cells shown in Fig. 4a. The initial volume of the pouch cells is 2.2 mL. A volume change during cycling less than 10% (0.22 mL) is desired. Fig. 4b shows all of the cells containing FEC:TFEC electrolyte (except 2% PES + 2%TAP, which has extremely high impedance) produce more gas during 500 h storage than cells containing EC:EMC or SL:EMC electrolyte. Simply increasing the amount of PES or adding TMS or TAP to FEC:TFEC electrolyte decreases the amount of gas evolution. These additives also limit gas evolution in EC:EMC electrolyte [36,37,46]. Adding MMDS increases the gas evolution. Fig. 4c shows the volume of gas produced during UHPC cycling for the same cells shown in Fig. 3. Fig. 4c shows control cells produce a large amount of gas during such aggressive charge-store-discharge protocols during UHPC testing. Fig. 4c shows that the gas evolution during UHPC cycling follows the same global trends as those in Fig. 4b during storage. That is, cells containing FEC:TFEC electrolyte produce more gas than EC:EMC or SL:EMC electrolytes.

Fig. 5a, b and 5c show a summary of the EIS data after formation, after 600 h UHPC cycling using the charge-store-discharge protocol and after the 500 h storage. EIS spectra for all of the cells containing FEC:TFEC 1:1 electrolytes tested in this study are given in Fig. S11. The EIS measurements were made at 3.80 V and at 10.0 ± 0.1 °C. Charge transfer resistance (R_{ct}) was calculated from the width of the semi-circle in the Nyquist representation of the electrochemical impedance spectra (see Fig. 2c). Fig. 5b and c shows that all cells containing FEC:TFEC electrolyte have a large impedance increase after UHPC cycling or storage tests while cells containing EC:EMC or SL:EMC electrolyte do not show this feature (compared with EIS data after formation in Fig. 5a). Fig. 5b and c shows that cells containing FEC:TFEC electrolyte have higher impedance after UHPC cycling or storage compared to cells with EC:EMC based electrolyte. Adding TAP, DTD, TMS or more PES to FEC:TFEC:2%PES electrolyte increases the impedance while adding MMDS, ES or TTSPi

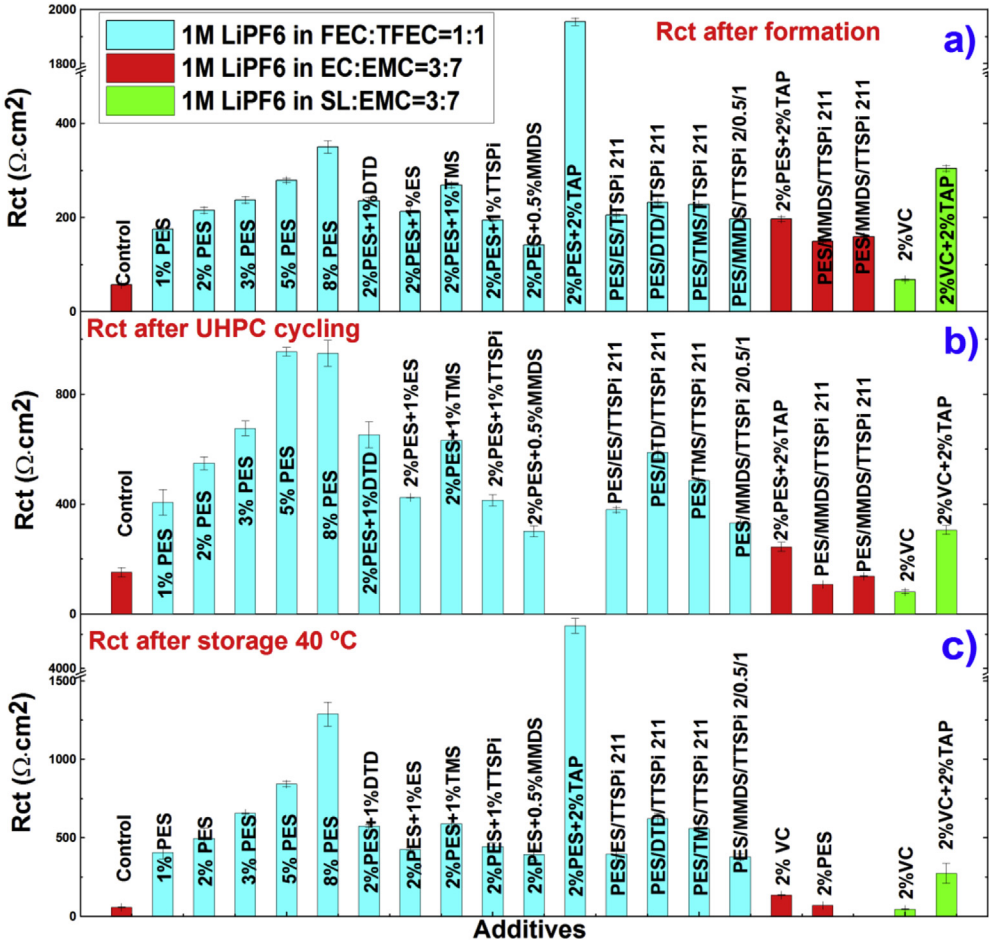

Fig. 5. Summary of the charge transfer resistance (R_{ct}) measured after a) UHPC cycling and b) 500 h storage at 40.0 °C for NMC442/graphite pouch cells containing FEC:TFEC, SL:EMC and EC:EMC electrolytes. The UHPC cycling/storage protocols are shown in Fig. S3.

decreases the impedance. Adding TAP to either FEC:TFEC or SL:EMC and EC:EMC electrolytes decreases the gas evolution during 500 h storage, however, the impedance after storage is simply too high, which is a strong disadvantage of the TAP additive [37].

Fig. 6a, b and c show the capacity versus cycle number for the NMC442/graphite pouch cells containing different additives combinations in FEC:TFEC, EC:EMC as well as SL:EMC electrolytes. All cells were continuously cycled with clamps to ensure firm pressure. Cells were cycled between 2.8 V and 4.5 V at 40 ± 0.5 °C using currents corresponding to C/2.4 (100 mA). A low rate C/10 cycle was included every 50 cycles to gauge what fraction of the capacity loss was due to impedance growth during the high rate cycling. Fig. 6d, e and f show the difference between average charge and discharge voltage, ΔV, vs cycle number for the same cells shown in Fig. 6a, b and c, respectively. Smaller values of ΔV indicate that cells have smaller polarization and lower DC resistance [45]. Results for only one cell are available due to a limited number of channels for this long-term testing. Fig. 6a and d shows that all cells containing FEC:TFEC:PES electrolyte have much better capacity retention and slower impedance growth rate than cells containing control electrolyte. Fig. 6a and d shows that adding more PES to FEC:TFEC electrolyte generally leads to worse capacity retention and larger ΔV during cycling. Fig. 6b and e shows that adding MMDS, DTD or TMS to FEC:TFEC:2%PES electrolyte improves the capacity retention while adding ES or TTSPi to FEC:TFEC-2%PES electrolyte decrease the capacity retention. Fig. 6c and f shows that adding TTSPi to the binary additive combinations does not obviously impact the capacity retention, however, it may lead to lower ΔV and better impedance control during cycling.

Fig. 7a gives the cycle number when the cell discharge capacity reaches 180 mAh (~80% capacity retention) for uncoated NMC442/graphite pouch cells containing different additive combinations in FEC:TFEC, SL:EMC and EC:EMC electrolytes. The cells were tested at 40 °C with C/2.4 currents and were cycled between 2.8 and 4.5 V. From left to the right, the cycle number to 80% capacity decreases indicating that cells on the left of Fig. 7a have the best cycle lifetime. Fig. 7a shows cells containing 1% PES, 2% PES + 1% DTD, 2% PES + 0.5% MMDS, 2% PES + 0.5% MMDS + 1%TTSPi or 2%PES + 1% DTD + 1%TTSPi in FEC:TFEC can cycle ~800 times (about 6 months testing) to 4.5 V with only 20% capacity loss which is pretty amazing.

Fig. 7b and c shows a summary of the EIS and volume change data collected after long-term cycling for the same cells shown in Fig. 7a. Compared with cells containing EC:EMC electrolytes, cells containing FEC:TFEC or SL:EMC electrolytes generally produced more gas during long-term cycling. Adding more PES decreases the gas generation in FEC:TFEC electrolyte which shows the same trend as the gas evolution data after UHPC cycling in Fig. 3c. Fig. 7c shows the impedance of cells containing FEC:TFEC electrolyte is very stable or even smaller after long-term cycling while the impedance of cells containing control or SL:EMC electrolyte increase a lot.

Fig. 8a shows R_{ct} after UHPC cycling (see Fig. 5b) plotted versus

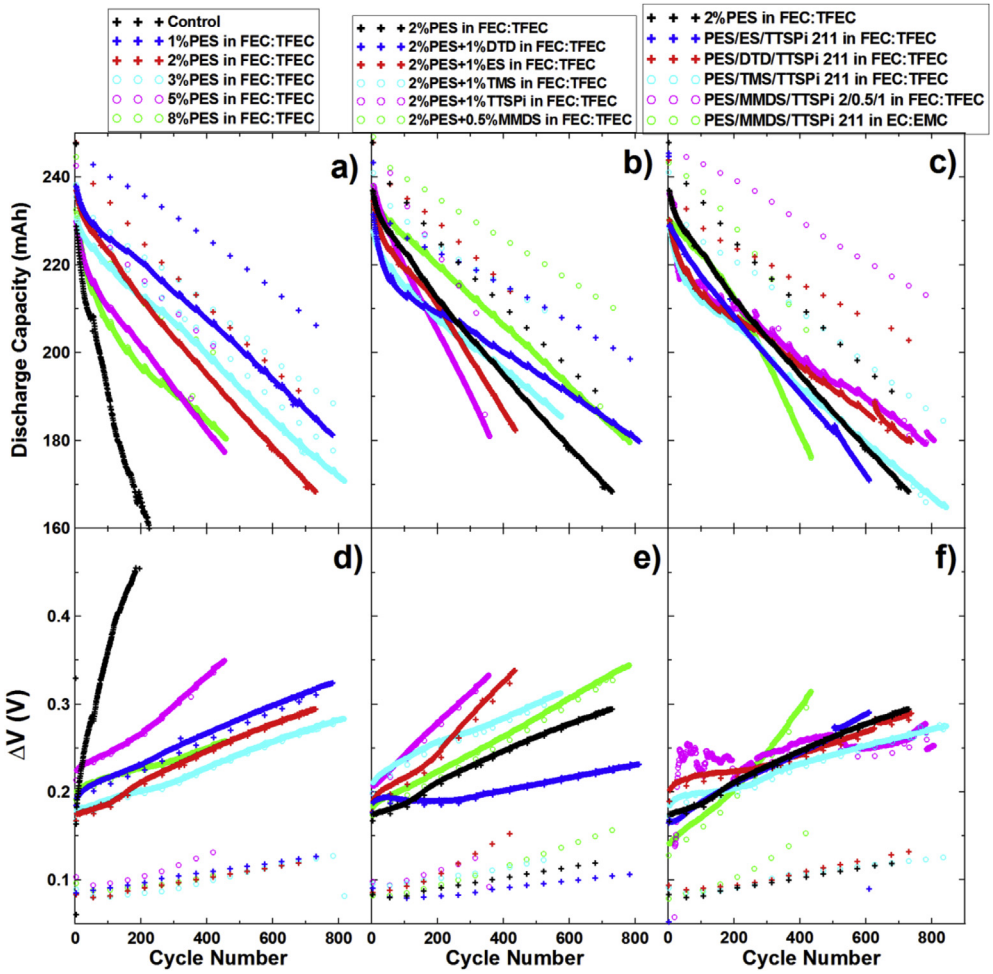

Fig. 6. a, b, c) Discharge capacity and d, e, f) ΔV, all plotted vs cycle number for NMC442/graphite pouch cells containing different kinds of electrolytes with different additive sets as indicated. The cycling was between 2.8 and 4.5 V at C/2.4 (100 mA) and 40.0 ± 0.1 °C using continuous cycling protocols.

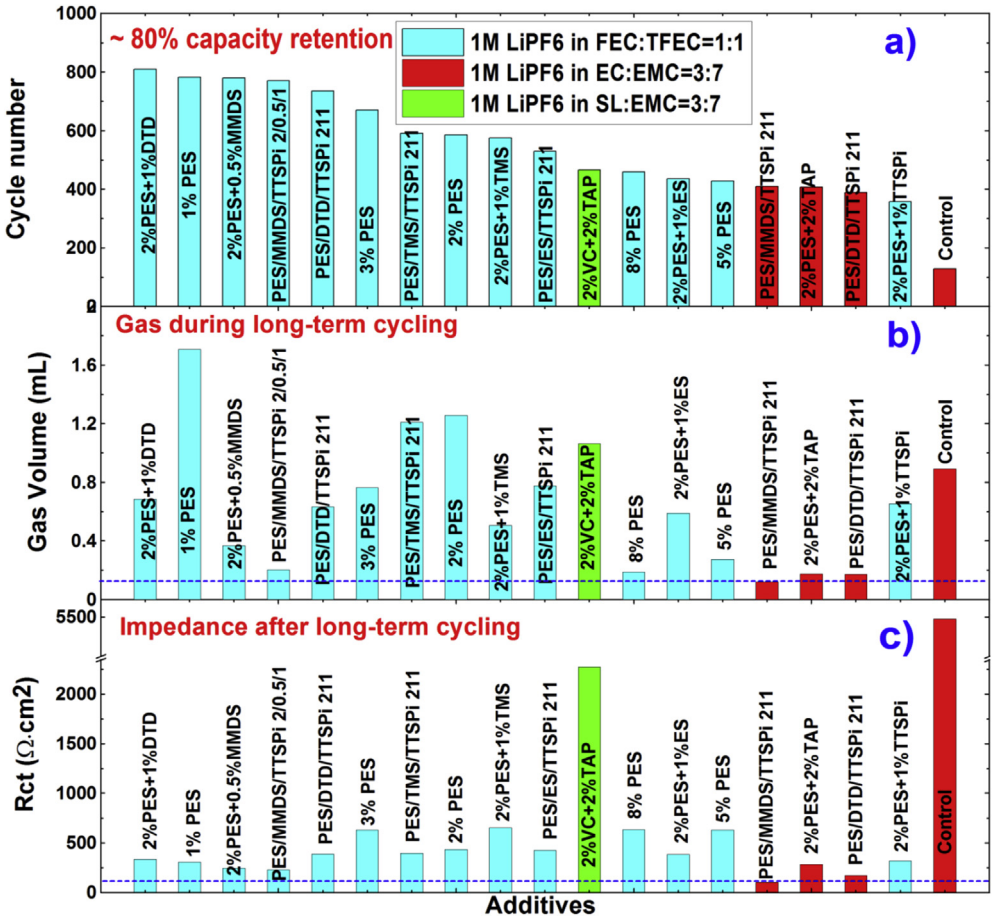

Fig. 7. a) The cycle number when the cell capacity reaches 180 mAh for NMC442/graphite pouch cells containing different kinds of electrolytes with different additive sets as indicated. The cycle number has been arranged from "best" in the left to "worst" in the right. The corresponding b) gas evolution during long-term cycling and c) R_{ct} after long-term cycling. The cycling was between 2.8 and 4.5 V at C/2.4 (100 mA) and 40.0 ± 0.1 °C using continuous cycling.

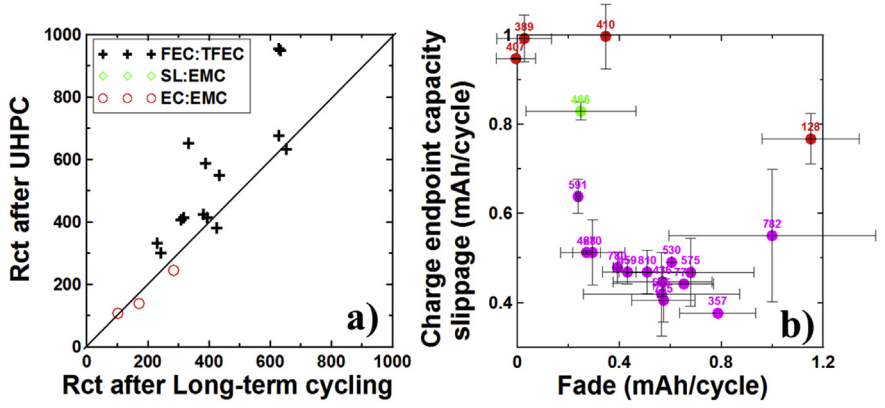

Fig. 8. a) R_{ct} after UHPC cycling (data in Fig. 5b) plotted versus R_{ct} after long-term cycling (data in Fig. 7c). b) Charge endpoint capacity slippage during UHPC cycling (data in Fig. 3c) plotted versus fade during UHPC cycling (data in Fig. 3b). The number above each data point in Fig. 8b is the cycle number when the cell capacity reaches 180 mAh during long-term cycling (data in Fig. 7a).

R_{ct} after long-term cycling (see Fig. 7c). Fig. 8a shows a good correlation between R_{ct} after UHPC cycling and R_{ct} after long-term cycling. Generally, cells with smaller R_{ct} after UHPC cycling also have the R_{ct} after long-term cycling.

Fig. 8b shows the charge endpoint capacity slippage during UHPC cycling plotted versus the fade rate during UHPC cycling. The number above each data point in Fig. 8b shows the cycle number when the cell capacity reached 180 mAh during long-term cycling (see Fig. 7a). Fig. 8b shows that cells containing EC:EMC or SL:EMC have a lower fade rate but much higher charge end-point capacity slippage (except for control cells, which have both high fade and high slippage) than cells containing FEC:TFEC electrolyte during UHPC cycling. Since all the cells were cycled with clamps during both UHPC cycling and long-term cycling, gas evolution during cycling will not impact the results in Fig. 8b. Apart from one pair of cells with 1% PES in FEC:TFEC tested on the UHPC (782 cycles to 80%

capacity indicated in Fig. 8b) the error bars in Fig. 8b are relatively small. Generally, the cells with the longest cycle life to 80% capacity are found in the lower left corner of Fig. 8b. If one of the cells with 1% PES in FEC:TFEC were excluded, then that data point (782 cycles) would move into the group of cells with long cycle life. Since the coulombic inefficiency, CIE, is related to the fractional charge endpoint capacity slippage per cycle, Δ_c/Q, and the fractional capacity fade per cycle, f/Q, by Ref. [47].

$$CIE = \Delta_c/Q + f/Q, \quad (2)$$

It is expected that cells in the lower left corner of Fig. 8b will have the longest cycle life. It must be pointed out that the UHPC testing, done under charge-store-discharge protocol to 4.4 V, and the long term cycling, done using continuous cycling to 4.5 V, were not the same. Therefore the correlation between UHPC testing and long term cycling are not expected to be perfect. Moreover, the long-term cycling was made at C/2 while the UHPC cycling was made at C/20. The huge impedance growth during high rate long-term cycling is hard to anticipate by the UHPC results collected during the low rate cycling.

Some of the data in Fig. 6 with FEC:TFEC electrolyte are very impressive. However, high impedance was normally observed. It is extremely important to compare the cycling performance of these fluorinated electrolytes and sulfolane-based electrolytes with other electrolytes with additives. Figs. S12a and S12b show the discharge capacity and **Δ**V, plotted vs. cycle number for NMC442/graphite pouch cells containing different kinds of electrolytes with selected electrolyte additive sets. The cycling was between 2.8 and 4.4 V at ~ C/1.6 (100 mA) and 19 ± 1 °C using continuous CCCV cycling protocols. These pouch cells were made by the same manufacturer but were from a different batch and therefore they had different cell capacities compared to the other cells used in this report. Methyl propionate (MP) was chosen because it can improve low temperature cycling performance [48,49]. Pyridine boron trifluoride (PBF)-based electrolyte additives was chosen because Nie et al. [50,51] showed that PBF delivered clear benefits in NMC442/graphite cells such as limiting the electrolyte oxidation as well as the impedance growth during storage and long-term cycling.

Fig. S12 shows that cells containing SL:EMC with 2%VC+2%TAP additive combinations have the worst capacity retention when tested at room temperature due to their high impedance. Fig. S12 shows cells containing PES211 or PES222 in EC:EMC:MP 21:49:30 electrolyte have the best cycling performance in NMC442/graphite pouch cells at room temperature. Fig. S12 shows cells containing 2% PES + 0.5%MMDS in FEC:TFEC electrolyte have good capacity retention and very little impedance growth in NMC442/graphite pouch cells.

4. Summary and conclusions

FEC:TFEC-based fluorinated electrolytes with electrolyte additives and their combinations were carefully studied in NMC442/graphite pouch cells. These were compared to the other two electrolyte systems including the "PES211" electrolyte additive blend in EC:EMC and a SL:EMC electrolyte with 2% VC + 2%TAP electrolyte additives. The results of CE, charge endpoint capacity slippage, changes in ΔV and V_{drop} during UHPC charge-store-discharge testing to 4.4 V and at 40 °C, V_{drop} during 500 h storage at 40 °C and 4.5 V, gas evolution, EIS as well as long-term cycling results were considered. Highlights of the work are:

1. Adding more PES (≥3%) to FEC:TFEC electrolyte leads to higher CE and less gas evolution. However, increasing the amount of PES greatly increased the impedance and shortened the cycle life during high rate long-term cycling.
2. The cycling performance of the FEC:TFEC:2%PES electrolyte system was affected by adding electrolyte additives. For example, adding DTD or MMDS increased the cycle life time while adding ES, MMDS or TTSPi decreased the impedance.
3. Compared with cells containing "PES211" in EC:EMC electrolyte or 2% VC + 2% TAP in Sulfolane:EMC electrolyte, cells containing FEC:TFEC-based electrolytes have higher CE and lower charge end-capacity slippage during UHPC charge-store-discharge cycling to 4.4 V and smaller voltage drop during storage periods.
4. Long term cycling tests (2.8 V - 4.5 V, 40 °C, C/2.4) show that cells containing FEC:TFEC-based electrolytes have much better capacity retention and less impedance growth, compared with cells containing "PES211" in EC:EMC electrolyte or 2% VC + 2% TAP in Sulfolane:EMC electrolyte. However, at 19 °C, cells with "PES211" in EC:EMC:MP electrolyte outperformed cells with fluorinated solvents presumably because of lower impedance and reduced rates of parasitic reactions at 19 °C compared to 40 °C.

This work confirms the benefits of using fluorinated electrolytes in high voltage Li-ion cells operated at elevated temperatures. By reducing the electrolyte oxidation at the positive electrode, FEC:TFEC electrolytes have smaller voltage drop during storage as well as a smaller charge endpoint capacity slippage rate during UHPC cycling. This is probably responsible for limiting the growth of cell polarization and impedance during cycling, leading to the better capacity retention. Electrolyte additives in FEC:TFEC electrolytes can help to reduce the gas evolution and decrease the impedance growth. However, the initial impedance, initial cell polarization and gas evolution during long-term cycling are still high when compared to EC:EMC electrolyte with appropriate additives. These problems appear to arise from the FEC:TFEC solvent blend itself and the electrolyte additives studied here cannot eliminate these problems entirely. The search for high voltage electrolytes for Li-ion cells must continue.

Acknowledgment

The authors acknowledge the financial support of NSERC and 3M Canada under the auspices of the Industrial Research Chairs program. The authors thank Dr. Jing Li of BASF for providing some of the solvents and salts used in this work. The authors thank Xiaodong Cao of HSC Corporation for providing the TFEC used in this work. Remi Petibon thanks NSERC and the Walter C. Sumner Foundation for Scholarship support.

Appendix A. Supplementary data

Supplementary data related to this article can be found at http://dx.doi.org/10.1016/j.jpowsour.2016.09.012.

References

[1] K. Abe, K. Miyoshi, T. Hattori, Y. Ushigoe, H. Yoshitake, J. Power Sources 184 (2008) 449.
[2] S. Santee, A. Xiao, L. Yang, J. Gnanaraj, B.L. Lucht, J. Power Sources 194 (2009) 1053.
[3] J.C. Burns, A. Kassam, N.N. Sinha, L.E. Downie, L. Solnickova, B.M. Way, J.R. Dahn, J. Electrochem. Soc. 160 (2013) A1451.
[4] J. Xia, L. Ma, J.R. Dahn, J. Power Sources 287 (2015) 377.
[5] L. Ma, J. Xia, J.R. Dahn, J. Electrochem. Soc. 161 (2014) A2250.
[6] J. Self, C.P. Aiken, R. Petibon, J.R. Dahn, J. Electrochem. Soc. 162 (2015) A796.
[7] R.P. Day, J. Xia, R. Petibon, J. Rucksa, H. Wang, J.R. Dahn, J. Electrochem. Soc. 162 (2015) A2557.
[8] K.J. Nelson, G.L. Eon, A.T.B. Wright, L. Ma, J. Xia, J.R. Dahn, J. Electrochem. Soc. 162 (2015) A1046.

[9] K. Xu, J. Electrochem. Soc. 145 (1998) 70.
[10] K. Xu, C.A. Angell, J. Electrochem. Soc. 149 (2002) 920.
[11] A. Abouimrane, I. Belharouak, K. Amine, Electrochem. Comm. 11 (2009) 1073.
[12] Y. Abu-lebdeh, I. Davidson, J. Electrochem. Soc. 156 (2009) A60.
[13] H. Duncan, N. Salem, Y. Abu-lebdeh, J. Electrochem. Soc. 160 (2013) 838.
[14] M. Nagahama, N. Hasegawa, S. Okada, J. Electrochem. Soc. 157 (2010) A748.
[15] K. Xu, C.A. Angell, J. Electrochem. Soc. 149 (2002) A920.
[16] M. Hu, X. Pang, Z. Zhou, J. Power Sources 237 (2013) 229.
[17] F. Wu, Q. Zhu, L. Li, R. Chen, S. Chen, J. Mater. Chem. A 1 (2013) 3659.
[18] Y. Watanabe, S. Kinoshita, S. Wada, K. Hoshino, H. Morimoto, S. Tobishima, J. Power Sources 179 (2008) 770.
[19] K.-C. Möller, T. Hodal, W.K. Appel, M. Winter, J.O. Besenhard, J. Power Sources 97–98 (2001) 595.
[20] M. Smart, B. Ratnakumar, V. Ryan-Mowrey, S. Surampudi, G.K. Prakash, J. Hu, I. Cheung, J. Power Sources 119–121 (2003) 359.
[21] Z. Zhang, L. Hu, H. Wu, W. Weng, M. Koh, P.C. Redfern, L.A. Curtiss, K. Amine, Energy Environ. Sci. 6 (2013) 1806.
[22] L. Hu, Z. Xue, K. Amine, Z. Zhang, J. Electrochem. Soc. 161 (2014) A1777.
[23] L. Hu, K. Amine, Z. Zhang, Electrochem. Comm. 44 (2014) 34.
[24] L. Hu, Z. Zhang, K. Amine, Electrochem. Comm. 35 (2013) 76.
[25] J. Xia, M. Nie, J.C. Burns, A. Xiao, W.M. Lamanna, J.R. Dahn, J. Power Source 307 (2016) 340.
[26] T.M. Bond, J.C. Burns, D.A. Stevens, H.M. Dahn, J.R. Dahn, J. Electrochem. Soc. 160 (2013) A521.
[27] N.N. Sinha, T.H. Marks, H.M. Dahn, A.J. Smith, J.C. Burns, D.J. Coyle, J.J. Dahn, J.R. Dahn, J. Electrochem. Soc. 159 (2012) A1672.
[28] C.P. Aiken, J. Xia, D.Y. Wang, D.A. Stevens, S. Trussler, J.R. Dahn, J. Electrochem. Soc. 161 (2014) A1548.
[29] D.Y. Wang, J. Xia, L. Ma, K.J. Nelson, J.E. Harlow, D. Xiong, L.E. Downie, R. Petibon, J.C. Burns, A. Xiao, W.M. Lamanna, J.R. Dahn, J. Electrochem. Soc. 161 (2014) A1818.
[30] J. Xia, Z. Lu, J. Camardese, J.R. Dahn, J. Power Sources 306 (2016) 516.
[31] D. Aurbach, K. Gamolsky, B. Markovsky, Y. Gofer, M. Schmidt, U. Heider, Electrochim. Acta 47 (2002) 1423.
[32] B. Li, M. Xu, T. Li, W. Li, S. Hu, Electrochem. Commun. 17 (2012) 92.
[33] J. Xia, J.E. Harlow, R. Petibon, J.C. Burns, L.P. Chen, J.R. Dahn, J. Electrochem. Soc. 161 (2014) A547.
[34] J. Xia, C.P. Aiken, L. Ma, G.Y. Kim, J.C. Burns, L.P. Chen, J.R. Dahn, J. Electrochem. Soc. 161 (2014) A1149.
[35] N.N. Sinha, J.C. Burns, J.R. Dahn, J. Electrochem. Soc. 161 (2014) A1084.
[36] J. Xia, N.N. Sinha, L.P. Chen, J.R. Dahn, J. Electrochem. Soc. 161 (2013) A264.
[37] J. Xia, L. Madec, L. Ma, L.D. Ellis, W. Qiu, K.J. Nelson, Z. Lu, J.R. Dahn, J. Power Sources 295 (2015) 203.
[38] J. Xia, J. Self, L. Ma, J.R. Dahn, J. Electrochem. Soc. 162 (2015) A1424.
[39] C.P. Aiken, J. Self, R. Petibon, X. Xia, J.M. Paulsen, J.R. Dahn, J. Electrochem. Soc. 162 (2015) A760.
[40] N.N. Sinha, A.J. Smith, J.C. Burns, G. Jain, K.W. Eberman, E. Scott, J.P. Gardner, J.R. Dahn, J. Electrochem. Soc. 158 (2011) A1194.
[41] R. Petibon, L. Madec, D.W. Abarbanel, J.R. Dahn, J. Power Source 300 (2015) 419.
[42] N.N. Sinha, J.C. Burns, J.R. Dahn, J. Electrochem. Soc. 161 (2014) A1084.
[43] J. Xia, M. Nie, L. Ma, J.R. Dahn, J. Power Source 306 (2016) 233.
[44] J.C. Burns, N.N. Sinha, G. Jain, H. Ye, C.M. VanElzen, W.M. Lamanna, A. Xiao, E. Scott, J. Choi, J.R. Dahn, J. Electrochem. Soc. 159 (2012) A1105.
[45] J.C. Burns, X. Xia, J.R. Dahn, J. Electrochem. Soc. 160 (2012) A383.
[46] J. Xia, L. Ma, C.P. Aiken, K.J. Nelson, L.P. Chen, J.R. Dahn, J. Electrochem. Soc. 161 (2014) A1634.
[47] A.J. Smith, J.C. Burns, D. Xiong, J.R. Dahn, J. Electrochem. Soc. 158 (2011) A1136.
[48] S.V. Sazhin, M.Y. Khimchenko, Y.N. Tritenichenko, H.S. Lim, J. Power Sources 87 (2000) 112.
[49] M.C. Smart, B.V. Ratnakumar, A. Behar, L.D. Whitcanack, J.S. Yu, M. Alamgir, J. Power Sources 165 (2007) 535.
[50] M. Nie, J. Xia, L. Ma, J.R. Dahn, J. Electrochem. Soc. 162 (2015) A2066.
[51] M. Nie, J. Xia, J.R. Dahn, J. Electrochem. Soc. 162 (2015) A1186.